

The influence of sample refraction in the X-ray LLL interferometer

JIE WU*, JIABI CHEN

School of Medical Instrument and Food Engineering, University of Shanghai for Science and Technology, Shanghai, 200093, P. R. China

An interferometry method based on the X-ray crystallography is explored to the measurement of refractive index, and a triple Laue-case(LLL) interferometer configuration is formed according to the dynamical theory of X-ray diffraction. Then several aspects about the X-rays refraction phenomenon originated by the sample, the deviation of the X-ray incident angle from the Bragg diffraction angle, and the shift distance of the exit point, are discussed to find the influence of analyzer parameters on the interference signal of the X ray LLL interferometer, and computer simulations are made to reveal the relationship between the analyzer thickness and the shift distance of the exit point, and an optimization scheme about the analyzer parameter are presented to improve the spatial resolution for the X- ray interferometer.

(Received May 5, 2014; accepted May 7, 2015)

Keywords: X-ray, Interferometer, Crystal, Refractive index

1. Introduction

The traditional X-ray CT images are created from the differences of X-ray absorption, however, many weak absorbing materials with low-Z elements are so difficult to observe, such object dose not absorb enough X-rays to create the contrast in its image[1,2]. In order to overcome this difficulty, we can use information of the X-rays phase variation that travels through the object, to form a phase contrast images or to develop a phase contrast CT.

In recent years many researches on the phase imaging techniques appeared in the X-ray region. The phase variation is caused by the spatial variation of refractive index for the X-ray in the object. Therefore the internal structure of the object is displayed as a distribution of refractive index for the X-ray[3,4]. Because the interaction cross section of the X-ray phase shift is over a thousand times larger than that of the X-ray absorption for low-Z elements, the X-ray phase contrast imaging is expected to be effective for observing those organic and biological materials, such as human soft tissues[5,6].

Recently a novel kind of refractive index interferometry method based on the X-ray crystallography is used in this technology, and the main configuration form is a triple Laue-case(LLL) interferometer according to the dynamical theory of X-ray diffraction[7,8]. In this LLL type of interferometer, Laue-case diffraction takes place in every wafer, when the incident X-ray beam exposures to the first wafer splitter, it produces two coherent beams. Then the second and the third wafer named mirror and analyzer recombine the interfering beams, and produce two outgoing beams.

When the X-ray wave passes through the sample inserted in one of the paths of coherent beams, the phase contrast is effectuated by local alterations of the X-ray refractive index in the sample. The phase shift caused by the sample, and the interference patterns appear in the forward beams. At the same time, the X-rays are slightly refracted by the sample, and the incidence angle of the X-ray beam to the analyzer deviates slightly from the diffraction conditions [9,10]. Therefore, the spatial resolution is restricted by this deviation, which is insufficient for applying the technology to practice.

In this paper, several fundamental issues about the interferometry method based on the X-ray crystallography will be discussed, it includes the refractive index and the detection methods, the optical design of the X-ray interferometry method, the specific analysis of the X-ray crystallography and so on. At last, several analyzer parameters are discussed to find the influence of analyzer parameters on the interference signal of the X ray LLL interferometer, and presents an optimization scheme of the analyzer parameters to improve the spatial resolution for the X- ray interferometer.

2. Materials and Methods

2.1. Absorption coefficient and refractive index

Both X-rays and visible rays are electromagnetic waves, the wavelength of X-rays described here is in the range around 0.1 nm, which corresponds to the photon energy larger than about 10 keV. For hard X-rays with

photon energy of 10 keV, refractive index of the ordinary material is smaller than that of vacuum by about 10^{-6} to 10^{-7} , Absorption coefficient and refractive index for the hard X-ray region has been shown in many papers[11,12]. The complex refractive index n is represented by

$$n = 1 - \delta + i\beta \quad (1)$$

Note that the refractive index is a little smaller than 1. The real part δ and imaginary part β are expressed by the phase-shift cross-section f_1 and the atomic absorption cross-section f_2

$$\delta = \frac{r_0 \lambda^2}{2\pi} N_A f_1 \quad (2)$$

$$\beta = \frac{r_0 \lambda^2}{2\pi} N_A f_2 \quad (3)$$

where N_A is the atomic density of the element, the f_1 and f_2 are varied by the elements of different atomic number. Materials of low atomic number show very little absorption coefficient, therefore the absorption contrast image is low for the object consisting of these elements. However, refractive index does not decrease remarkably with atomic number compared with absorption. For instance, the values of δ and β of water are 5.8×10^{-7} and 6.0×10^{-10} for 20 keV X-rays. The ratio δ/β is about 10^3 for 20-keV X-ray as shown in table 1. This indicates that materials with a low absorption coefficient can be imaged without any staining.

Table 1. Comparison of phase term and absorption term of some low-Z materials

Materials	δ	β
Polyethylene	5.0×10^{-7}	3.2×10^{-10}
water	5.8×10^{-7}	6.0×10^{-10}
glass	1.3×10^{-6}	2.9×10^{-9}
silicon	1.2×10^{-6}	4.9×10^{-9}
iron	3.8×10^{-6}	9.7×10^{-8}

2.2. X-ray interferometry method

In the X-ray region, similar interferometer was devised about 40 years ago, it is the Bonse–Hart type interferometer. As there is no adequate mirror in the X-ray region, Bragg diffraction by a single Si crystal is used for dividing the X-rays. The interferometer consists of three Si blades S, M, A and their base, which is shown in the Fig.1. Whole interferometer is made monolithically from a Si single crystal. The lattice plane diffracting the X-ray is

perpendicular to the blade surface. If a X-ray is incident on the first blade S in the direction satisfying the Bragg condition, the ray is divided into diffracted ray and penetrating ray. Both rays reach the blade M, where they are diffracted again. The two diffracted rays coincide on the blade A, where one of them is diffracted and the other penetrate through the blade. Recently, this type of interferometer has been used for phase imaging and refractive index tomography.

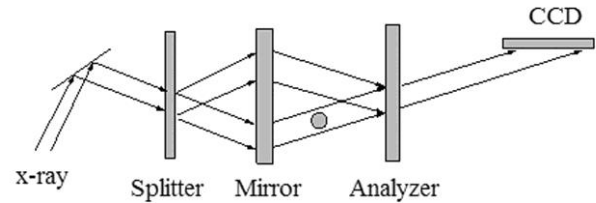


Fig.1 X-ray interferometry method based on the crystallography. The LLL interferometer consists of three Si blades Splitter, Mirror, Analyzer.

In this interferometry method, In order to adopt the phase-shifting method, an acrylic wedges is inserted into one of the arms as a phase shifter, as shown in Fig.1. The wedge is rotated around the axis perpendicular to the apex line. The rotation brings different phase change to the two interfering beams because they penetrate the wedge with different thickness.

When the phase of the object beam is denoted by $\phi(X, \xi)$, the intensity variation of the interfered beam is expressed as

$$I(X, \xi) = I_a(X, \xi) + I_b(X, \xi) \cos(\phi(X, \xi) + \Phi) \quad (4)$$

Where Φ is phase difference caused by the path length difference between the two arms without the object. $I_a(X, \xi)$ and $I_b(X, \xi)$ are determined by the intensity of the two interfering beams. From this expression, phase change can be detected by counting the peak of the intensity variation.

X-rays in one arm is the reference beam, the other beam penetrate the object. The interfered beam intensity variation is expressed in the same equation as equation 4. But there are some factors of the interferometer will affect the clarity and contrast of the final interference signal.

2.3 The deviation due to the refraction of sample

In the interferometer, X-rays diffraction in each single crystal can be treated according to kinematical or dynamical theory. The condition for diffraction in a crystal is fulfilled when the angle between the incident X-ray beam and the crystal net planes equals the Bragg angle θ_b , which is defined by $2d\theta_b = n\lambda$.

In most cases it is possible to employ pairs of equivalent mirrors which affect the amplitudes of the two interfering beams symmetrically. Hence, to ensure $I_a = I_b$ over the full range, the analyzer must have the same thickness as the beam splitter and transmit the beam

previously reflected in the splitting process and vice versa. Consequently only one of the beams emerging from the analyzer can usually reach high contrast.

At the same time, X-rays are also refracted slightly by the sample, in this refraction phenomenon, the X-ray beam incidence angle to the analyzer will deviate slightly from the Bragg angle[13]. The deviation angle on the analyzer, $\Delta\theta$, which is originated by the sample refraction, is rarely mentioned in the early literatures, but the deviation angle can amount to several arcseconds in some cases. According to the dynamical theory of the X-ray diffraction, the deviation angle θ_{out} between the energy flow direction and the lattice plane is given by the equation 5

$$\theta_{out} = \tan^{-1} \left(\frac{W^2 - W\sqrt{W^2 + 1}}{1 + W^2 - W\sqrt{W^2 + 1}} \tan\theta_b \right) \quad (5)$$

The symbol W in equation 5 is expressed as equation 6

$$W = \frac{\pi V \sin 2\theta_b}{\lambda^2 r_e |P| |F_h|} \Delta\theta \quad (6)$$

In the two equations P is the polarization factor, F_h is the crystal structure factor, V is the volume of the unit cell, r_e is the classical electron radius.

When the x-ray beam exits the analyzer, the distance D from the actual exit point to the ideal exit point for $\Delta\theta = 0$, is calculated by equation 7

$$D = t_a |\tan\theta_{out}| \quad (7)$$

In this equation t_a is the thickness of the analyzer, θ_{out} is the deviation angle caused by the diffraction in the sample.

3. Results

To investigate the clarity and contrast of the final interference signal of the X-ray interferometer, we perform a computer simulation according to the theoretical analysis formula above. The aim is to find the spatial resolution variety due to diffraction of the sample itself and the analyzer, the simulation results can provide an experimental basis for the scientific and reasonable design of the interferometer.

The computer simulation conditions are: the Laue-case Si 220 diffraction, $P = 1$, $\lambda = 0.07\text{nm}$, The calculation result is shown in the Fig.2, which is the

deviation angle θ_{out} of the X-ray propagation direction outside the crystal caused by the deviation $\Delta\theta$ of the X-ray incident angle from the Bragg diffraction angle. It can be seen that a small deviation $\Delta\theta$ of the X-ray incident angle is amplified many times by the crystal diffraction. Because the samples have complex three dimensional structures, the diffraction blurring effect remains to some extent, and this factor limits the current spatial resolution of the X-ray phase contrast imaging technology.

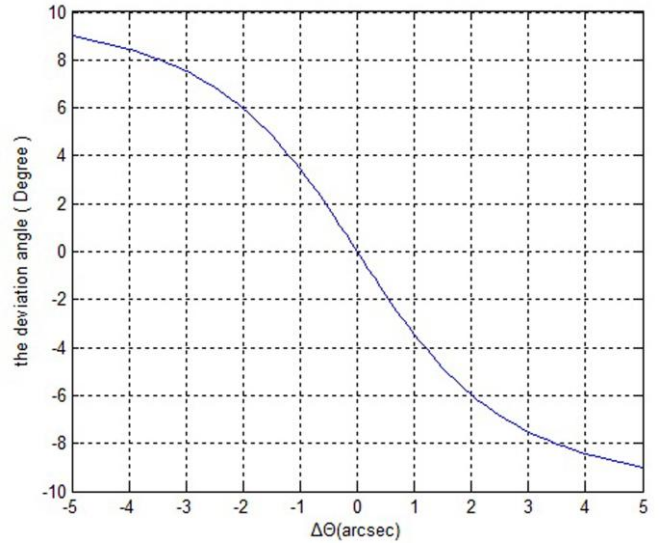


Fig.2. the deviation angle θ_{out} changed with the $\Delta\theta$ caused by the refraction in sample. a small deviation of the X-ray incident angle is amplified many times by the crystal diffraction.

Another factor that will influence the interference signal resolution is the analyzer thickness in the interferometer. When the refracted beam by the sample and the non-refracted reference beam interfere, the interference fringes are produced, and the fringes period is governed by $\lambda/\Delta\theta$. For a certain analyzer thickness parameter, it has a corresponding shift distance D of the exit point. Because the point shift distance must be smaller than the fringes period, so it has the relation $D < |\lambda/\Delta\theta|$.

In this computer simulation, calculations are performed for $t_a = 70\mu\text{m}$, $t_a = 250\mu\text{m}$ and $t_a = 1\text{mm}$, and under the same condition as above: the Laue-case Si 220 diffraction, $P = 1$, $\lambda = 0.07\text{nm}$. The simulation results are shown in the Fig.3, the shift distance of exit point changed with the deviation $\Delta\theta$ of the X-ray incident

angle from the Bragg diffraction angle.

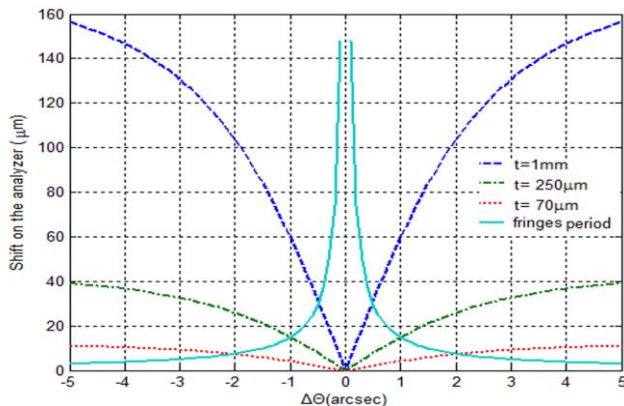


Fig.3. the shift distance of exit point for different thickness of the analyzer comparing with the fringes period. Calculations conditions are: the Laue-case Si 220 diffraction, $P=1$, $\lambda=0.07$ nm.

From the Fig.3, we can see that the thickness of the analyzer can affect the X-ray exit point dramatically. As a result, the visibility of the interference fringes decreases and the spatial resolution degrades very much. Because the shift does not occur in the perpendicular direction to the scattering plane, the rotation axis of a sample should set parallel to the scattering plane, which can let the blurring effect minimum.

To improve the resolution of the interference model and to broaden the valid region for $\Delta\theta$, we can fabricate the X-ray interferometer with a thin analyzer. It can be seen from the Fig. 3 that the valid region of $\Delta\theta$ is between $-0.5''$ and $+0.5''$ for $t_a = 1\text{mm}$, $\Delta\theta$ is between $-1''$ and $+1''$ for $t_a = 250\mu\text{m}$, and $\Delta\theta$ is between $-2''$ and $+2''$ for $t_a = 70\mu\text{m}$.

4. Discussion

Among various refractive index interferometry methods developed over the last decades, the triple Laue case interferometer excels by its broad spectrum of applications, and the other types remained in the stage of instrument testing. The observations and discussions in this paper are concluded with the following remarks:

(1) The deflection angle of X-ray propagation direction outside crystal caused by the deviation $\Delta\theta$ of the X-ray incident angle from the Bragg diffraction angle, is amplified roughly 10^4 times by the last analyzer

crystal in the X-ray interferometer. It suggests that the sample will be not too thick, because the deflection originated from the diffraction inside of the sample, can change the deviation $\Delta\theta$ of the X-ray incident angle from the Bragg diffraction angle, and this would end up producing fuzzy on the final interference signal.

(2) The thickness of analyzer crystal in the X-ray interferometer is an important parameter, further thinning of the analyzer, easier to produce clear signals. Because large deviation $\Delta\theta$ of the X-ray incident angle from the Bragg diffraction angle can be accepted with clear interference fringes, and the sample which causes lesser refraction can be observed with better resolution.

(3) If the thickness of analyzer crystal is fitted, then we have to improve the spatial coherence of light source, which can reduce the deviation $\Delta\theta$ of the X-ray incident angle from the Bragg diffraction angle, and then reduce the burring of the final interference signal. To improve the resolution of the interference model and to broaden the valid region for $\Delta\theta$, we can fabricate the X-ray interferometer with a thin analyzer. It can be seen from the Fig. 3. that the valid region of $\Delta\theta$ is between $-0.5''$ and $+0.5''$ for $t_a = 1\text{mm}$, $\Delta\theta$ is between $-1''$ and $+1''$ for $t_a = 250\mu\text{m}$, and $\Delta\theta$ is between $-2''$ and $+2''$ for $t_a = 70\mu\text{m}$

Currently, the X-ray phase-contrast imaging or X-ray refractive index measurement with interferometer has been carried out for biological soft tissues or materials consisting mainly of low-Z elements, without the need of staining. But the extraordinary deflection of X-ray inside the crystal and the sample is a main limiting factor to the spatial resolution of the X-ray interferometer. We have explored the theory and carried out simulation tests, to interpret the influence of analyzer parameters on the interference signal of the X-ray LLL interferometer.

Acknowledgments

This work was supported by the National Natural Science Foundation of China (61101174), and the Shanghai College Teacher Production Studying and Researching Practice Program.

References

- [1] C.C. Chien, P.Y. Tseng, H.H. Chen, *Biotechnology Advances*, **31**, 375 (2013)
- [2] Ewelina Kosior, Sylvain Bohic, Heikki Suhonen, *Journal of Structural Biology* **177**, 239 (2012)
- [3] Xiaoxu Lu, Jianpei Chen, Shengde Liu, *Optics and Lasers in Engineering*, **50**, 1431 (2012).

-
- [4] Huaying Zhao, Patrick H. Brown, and Peter Schuck, *Biophysical Journal*, **100**, 2309 (2011).
- [5] R. Heine, T.Gorniak, T.Nisius, C.Christophis, *Ultramicroscopy*, **111**, 1131 (2011).
- [6] Akio Yoneyama, Tohoru Takeda, Yoshinori Tsuchiya, *App. Opt.* **16**, 3258 (2005).
- [7] Shu-Ang Zhou, Anders Brahme, *Physica Medica*, **24**, 129 (2008).
- [8] Chika Honda, Hiromu Ohara, *European Journal of Radiology*, **8**, 69 (2008).
- [9] Zhi-Feng Huang, Ke-Jun Kang, Li Zhang, *Phy. Rev. A* **79**, 13 (2009).
- [10] Fanbo Meng, Da Zhang, Xizeng Wu, *Optics Communications*, **282**, 3392 (2009).
- [11] A.Olivo, L.Rigon, S.J.Vinnicombe, *Applied Radiation and Isotopes*, **69**, 1033 (2009).
- [12] Keiichi Hirano, Atsushi Momose, *Japanese Journal of Applied Physics*, **38**, 1556 (1999).
- [13] Atsushi Momose, Keiichi Hirano, *Japanese Journal of Applied Physics*, **38**, 625 (1999).

*Corresponding author: wujie3773@sina.com